

**SYNTHESIS, STRUCTURE AND OPTICAL PROPERTIES OF ZN DOPED TIN OXIDE****J. R. Sheeba*¹, S. Radhika², C. M. Padma¹**¹Research Scholar, (Reg. No: 17223282132013), Department of Physics, Women's Christian College, Nagercoil, Affiliated to Manonmanium Sundaranar University, Abishekapatti, Tirunelveli, India²Department of Physics, Pioneer Kumaraswamy College, Nagercoil*Corresponding author: jrsheeba@rediffmail.com**ABSTRACT**

Pure Tin oxide (SnO₂) and zinc doped tin oxide are prepared by co-precipitation method. The structural and optical properties are characterized by using XRD, SEM, FTIR, and UV-Visible techniques. The energy dispersion X-ray spectroscopy (EDAX) measurement estimates the elemental composition. The Powder XRD analysis confirms the tetragonal (rutile) structure of the nano crystals. The crystallite size and morphology of the nano particles are studied using scanning electron microscopy. The Functional group is identified using FTIR analysis. As the crystallite size increases, the band gap of Zinc doped Tin oxide nano particles shifts from 3.99eV to 3.839eV.

Keywords: Co-Precipitation Method, Crystallite Size, Optical Band Gap**1. INTRODUCTION**

One dimension nano scale materials have gained many scientists attention due to their unique electronic, optical and mechanical properties. Semi conducting oxide materials show the properties such as super conductivity, ferro electricity, magnetism etc., covering all the aspects of material science. High transparency semi conductor such as SnO₂ and ZnO have potential applications in catalysis, gas sensing, opto electronics and solar cells [1-4] etc. Tin oxide, cassiterite structure is an n-type semi conductor with a band gap of 3.6eV-3.8eV [5-7]. A number of studies have been performed dealing with various properties on SnO₂ nano materials. Furthermore, previous studies suggested that doping on tin oxide nano structure with transition metals enhance their activity by change in band structure of tin oxide [8-10].

Various techniques have been reported for the synthesis of tin oxide nano particles including, micro wave technique, solvo thermal, hydro thermal, sono chemical, mechano chemical, co-precipitation etc. [11-17]. Of these techniques, in the present work, co-precipitation has been employed because it is simple, inexpensive, does not require high temperature and pressure. In this method the size of the particle can be controlled by altering pH of the medium, concentration of precursor and precipitating reagents. Impurities in the precipitate are easily eliminated by filtration and repeated washing.

The particles have been characterized by means of XRD, FTIR, UV-Vis, SEM and EDAX.

2. EXPERIMENTAL, RESULTS AND DISCUSSION**2.1. Preparation of pure and zinc doped tin oxide nano particles**

Analytical grade reagents were used for the synthesis of the sample. Tin chloride(IV) penta hydrate (SnCl₄.5H₂O, Sigma Aldrich), was used as starting material. Zinc chloride, EDTA, Sodium hydroxide and ethyl alcohol were used to prepare zinc doped tin oxide nano particles.

For the preparation of pure tin oxide and zinc doped tin oxide, 1M of Tin Chloride (IV) Penta hydrate (SnCl₄.5H₂O, Sigma Aldrich), was dissolved in 50 ml of deionised water in a 250 ml conical flask with constant stirring, later (0.1M) zinc chloride is added to another 50ml of Tin Chloride solution at room temperature under stirring to produce a transparent colloidal solution. 0.6 gm of EDTA was used as surfactant. Aqueous NaOH (1M) was slowly added drop wise to the resulting solutions in order to modulate the pH at 3 uniformly throughout the reaction. The colloidal solutions were then left for constant stirring for about 5 hours. The temperature was maintained at 60°C. White precipitates were formed. The precipitates were collected, filtered using Whatman filter paper and washed with de-ionized water several times until the effluents pH was neutral and

then with ethyl alcohol. After drying at 170°C in hot air oven for 2 hours, pure and zinc doped tin oxide nano particles were obtained.

2.2. Characterization techniques

2.2.1. XRD Analysis

The determination of crystallite size and phase were carried out using X’Pert Pro X-ray diffractometer (CuKα target, =15418 Å). XRD data were collected in the 2θ range of 20°–80° and the diffraction pattern of pure and zinc doped tin oxide are shown in figure 1. The diffraction peaks are in harmony with JCPDS card no: 88-0287 with a=4.737 Å and c=3.186 Å, and it belongs to tetragonal rutile structure. The major peaks appear at 2θ values 26.98°, 51.88° and 65.08° for tin oxide and the additional peak at 34.92° suggests the incorporation of zinc in tin oxide [18]. The cell parameters, for tin oxide are a = 4.81974Å and c = 3.06311Å and for zinc doped tin oxide are a =4.75604Å and c =3.20806Å and cell volume V =71.1557Å³ for tin oxide and for zinc

doped tin oxide V =72.5661Å³ was calculated using the formula:

$$1/d_{hkl}^2 = (h^2+k^2)/a^2 + l^2/c^2$$

Where, h, k, l miller indices and d_{hkl} is the distance between two consecutive planes (m=1) with plane index (hkl) and the unit cell volume of the Tetragonal system is, V=a²c. The crystallite size, D, was estimated from the peak width with the Scherrer’s formula [19].

$$D = (K\lambda) / (\beta\cos\theta_B)$$

Where, λ is X-ray wavelength β is the full width half maximum (FWHM) of a diffraction peak θ_B is the diffraction angle and K is the Scherrer’s constant (0.9).

The average crystalline size of tin oxide nano particles using Scherrer’s formula was 6.365 nm and the average crystallite size of zinc doped tin oxide was 6.2708 nm. It was found that the particle size decreases with the zinc dopant, which indicates that the doping can inhibit growth of the particles. Calculated parameters are given in the table 1.

Table: 1 Crystal Parameters

Sample details	Lattice constants (Å)		Crystallite size	
	Calculated	Standard	D=(Kλ)/(βcosθ _B) (nm)	Unit cell volume V (Å ³) ³
Pure SnO ₂	a =4.81974Å c=3.06311Å	a=4.737Å c=3.186Å	6.365 nm	71.1557Å ³
Zinc doped SnO ₂	a =4.75604Å c =3.20806Å		6.2708 nm	72.5661Å ³

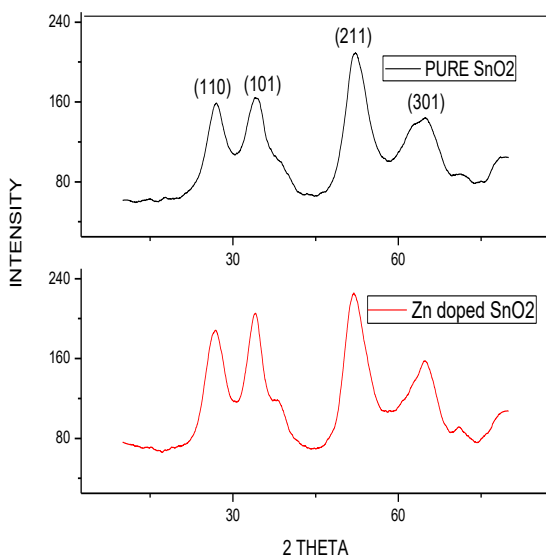


Fig. 1: XRD pattern of pure and zinc doped tin oxide nano particles

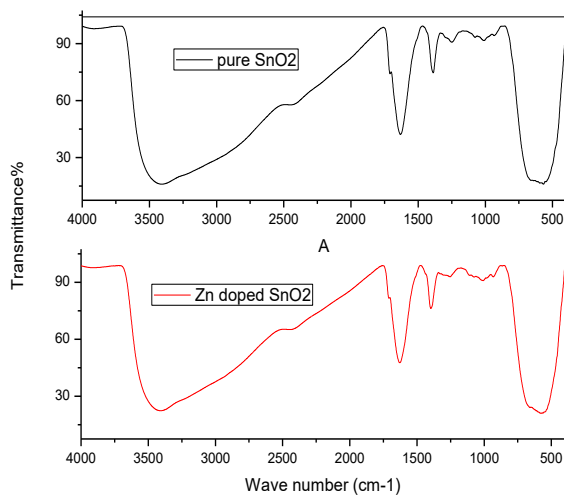


Fig. 2: FTIR pattern of pure and zinc doped tin oxide

2.2.2. FTIR Spectrum

The FTIR spectrum of the synthesized sample is shown in figure 2. The strong broad peak centred at 640.16 cm^{-1} corresponds to Sn-O-Sn stretching vibration. The band at 550 cm^{-1} is attributed to stretching modes of Sn-OH. The broad envelope in the higher energy region about 3400 cm^{-1} and 1707 cm^{-1} were due to stretching vibrations of water molecules absorbed at the surface of the tin oxide. However, the peak at 640.16 cm^{-1} is assigned to SnO_2 vibration thus confirming that the obtained precipitate is SnO_2 .

2.2.3. UV-Visible Spectrum

The UV-Vis absorbance of tin oxide and zinc doped tin oxide nano crystallites are shown in figure 3. The characteristic absorption peak was found around 310 nm for pure tin oxide and 322 nm for zinc doped tin oxide. From the analysis of the transmittance peaks of tin oxide and zinc doped tin oxide the energy gap is found to be 3.99eV and 3.839eV respectively. These values are found to be shifted when compared with the reported values of the bulk 3.6eV and 3.37eV for SnO_2 and ZnO respectively [1, 20]. It should be noted that doping slightly enhances the transmission indicating good incorporation of the dopant in the SnO_2 lattice structure.

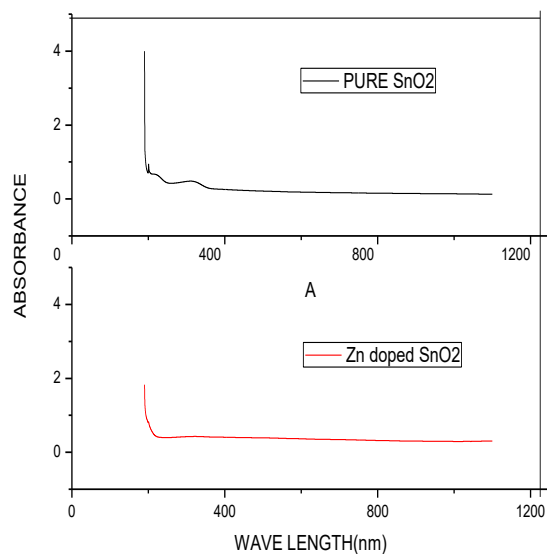


Fig. 3: Absorbance Spectrum of pure and zinc doped tin oxide

2.3.4. SEM Analysis

Pure tin oxide and zinc doped tin oxide are synthesized by co-precipitation method and the morphology and microscopic structure are characterized by using Scanning Electron Microscope (SEM) as shown in fig. 4

and fig.5. In the present study, the synthesized tin oxide is stabilised in tetragonal phase. When the crystallite size exceeds certain size, transformation of tetragonal to monoclinic can be observed. But no such phase transformation could be observed. The SEM analysis depicts the tetragonal arrangement of atoms. The SEM of Zinc doped tin oxide nano crystals show well defined structure than pure SnO_2 .

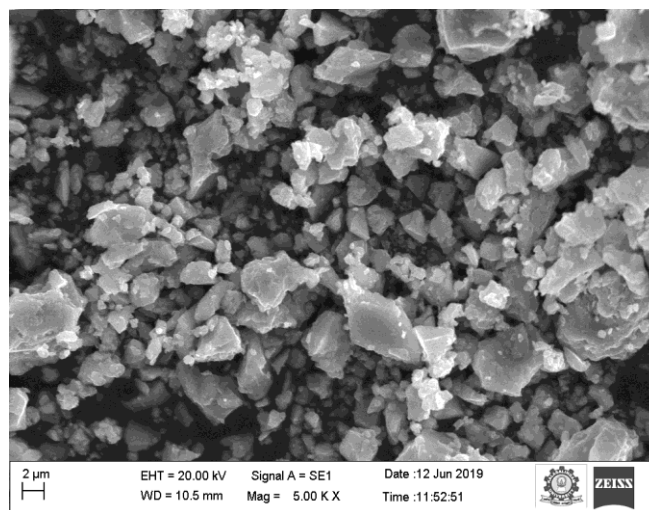


Fig. 4: SEM images of tin oxide

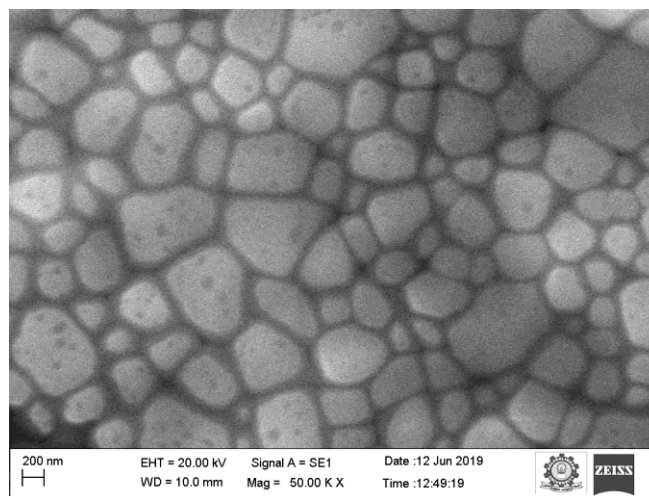


Fig. 5: SEM images of zinc doped tin oxide

The EDAX spectrum confirms the presence of Sn and O elements of the synthesised compound which is shown in the figure 6, also the figure 7 confirms the presence of Sn, O and Zn. The EDAX spectrum also confirms the absence of impurities that arise from the precursor and during the synthesis process. The atomic percentages of Sn and O elements present in the as-prepared powder are 74 and 26 mass%, respectively, and Sn, O and Zn

are 69,26 and 5 mass% respectively, which indicates that the synthesised SnO₂ powder and Zn doped SnO₂ is very close to the stoichiometry.

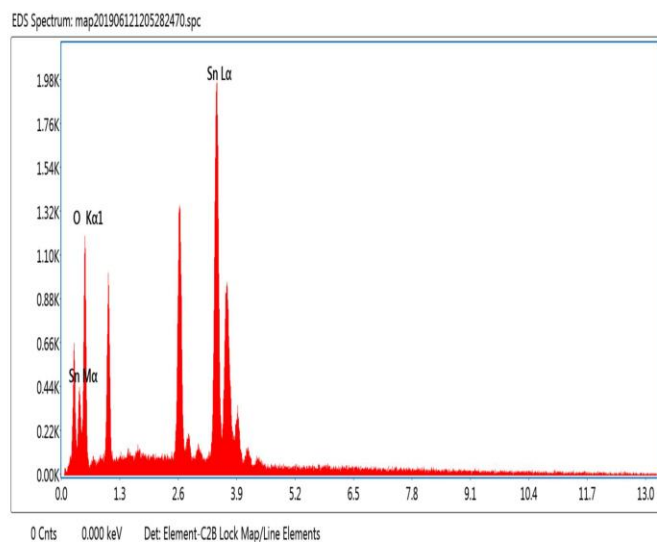


Fig. 6: EDX spectrum of pure tin oxide

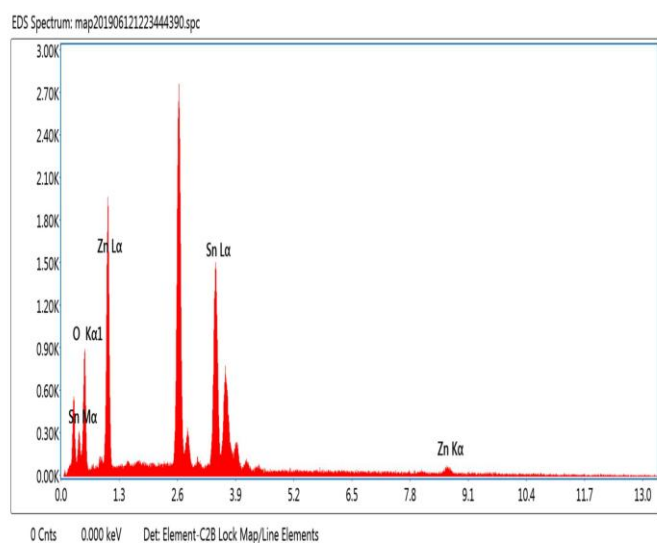


Fig. 7: EDX spectrum of zinc doped tin oxide

3. CONCLUSION

Pure tin oxide and zinc doped tin oxide nano particles have been synthesized by co-precipitation method. The samples were characterized by XRD, FTIR, UV-Vis, SEM and EDAX. The powder XRD pattern indicates the crystalline nature of the sample. The crystallite size was determined from Scherrer formula. The crystallite size was found to be 6.365nm for tin oxide and 6.2708 nm for zinc doped tin oxide. In the FTIR spectra, the peak at 640cm⁻¹ indicates the presence of tin oxide. The optical band gap was determined to be 3.99eV for tin oxide and 3.8399eV for zinc doped tin oxide from absorption

spectrum. From the SEM analyses it can be observed that the particles are finer and possess well define crystal morphology than pure one. The presence of Zn ions enhances the optical behaviour and decreasing band gap and so it is suitable for functional/active devices.

4. REFERENCES

1. Bahade ST, Lanje AS, Sharma SJ. *IJSRST*, 2017; **3(7)**:567-575.
2. Lanje AS, Sharma SJ, Pode RB. *LAMBERT Acad. Pub.,Germany*, 2014.
3. Lanje AS, Ningthoujam RS, Sharma SJ, Pode RB. *Ind. J. of Pure & App. Phys.*, 2011; **49**:234-238.
4. Yang HY, Yu SF, Liang HK, Lau SP, Pramana SS, et al. *Appl. Mater. Interfaces*, 2010; **2(4)**:1191-1194.
5. Gu F, Wang SF, Lu1 MK, Zhou GJ, Xu D, Yuan DR. *J. Phys. Chem. B.*, 2004; **108**:8119-8123.
6. Rahman IA, Vejayakumaran P, Sipaut CS, Ismail Abu Bakar M, Adnan R, Chee CK. *Ceram. Int.*, 2006; **32**:691-699.
7. Ren Y, Zhao G, ChenY. *Appl. Surf. Sci.*, 2011; **258**:914-918.
8. Xu C, Tamaki J, Miura N, Yamazoe N. *Sens Actuators B*, 1991; **3**:147-155.
9. Zhang G, Liu M, *Sens Actuators B.*, 2000; **69**:144-152.
10. Caihong W, Chu XF, Wu MM. *Sens Actuators B.*, 2007; **120**:508-513.
11. Shek CH, Lai JKL, Lin GM. 1999; **11**:887-893.
12. Krishnakumar T, Nicola Pinna, Prasanna Kumari K, Perumal K, Jayapraksh R. *Mater. Lett.*, 2008; **62**:3437-3440.
13. Zhaohui Han, Neng Guo, Fanqing li, Wangqun Zhang, Huaquiao Zhao, Yitai Qian. *Mater. Lett.*, 2001; **48**:99-103.
14. Zirong Lia, Xueliang Lia, Xiaoxi Zhanga, yitao Qianc. *J.Crystal Growth*, 2006; **291**:258-261.
15. Xian,Luo Hu, ying-Ji Shu, Shi- Wei Wang. *Mater. Chem. and Phys.*, 2004; **88**:421-426.
16. Cukrov LM, Mc Cormick PG, Galatsis K, Wlodarski W. *Sens.Acturators B.*,2007; **77**:491-495.
17. Dabin Yu, Debao Wang, Weichao Yu, Yitai Qian. *Mater. Lett.*, 2006; **58**:84-87.
18. Bedia FZ, Bedia A, Aillerie M, Maloufi N, Benyoucef B. *Energy procedia.*, 2015; **74**:539-546.
19. Taylor A. *X-ray Metallography*, John Wiley, New York, 1961; 678-686.
20. Lanje AS, Sharma SJ, Pode RB and Ningthoujam RS. *Arch.Appl. Sci. Res.*, 2010; **2(2)**:127-135.